Wave normal directions and wave distribution functions for ground-based transmitter signals observed on GEOS-1

François Lefeuvre, T. Neubert, Michel Parrot

CENTRE NATIONAL D'ETUDES DES TELECOMMUNICATIONS

CENTRE NATIONAL DE LA RECHERCHE SCIENTIFIQUE

CENTRE DE RECHERCHES EN PHYSIQUE DE L'ENVIRONNEMENT TERRESTRE ET PLANETAIRE

CRPE

NOTE TECHNIQUE
CRPE /99

WAVE NORMAL DIRECTIONS AND WAVE DISTRIBUTION FUNCTIONS FOR GROUND-BASED TRANSMITTER SIGNALS OBSERVED ON GEOS-1

By
F. LEFEUVRE T. NEUBERT and M. PARROT

C.R.P.E./G.E.S.
45045 ORLEANS CEDEX

DANISH SPACE RESEARCH INSTITUTE
2800 LYNGBY DENMARK.

CENTRE NATIONAL D'ETUDES
DES TELECOMMUNICATIONS

CENTRE NATIONAL DE
LA RECHERCHE SCIENTIFIQUE

CENTRE DE RECHERCHES EN PHYSIQUE DE
L'ENVIRONNEMENT TERRESTRE ET PLANETAIRE

NOTE TECHNIQUE CRPE/99

WAVE NORMAL DIRECTIONS AND WAVE DISTRIBUTION FUNCTIONS FOR GROUND-BASED TRANSMITTER SIGNALS OBSERVED ON GEOS-1

by

F. LEFEUVRE[1], T. NEUBERT[2] and M. PARROT[1]

1. C.R.P.E./G.E.S.
45045 ORLEANS CEDEX

2. DANISH SPACE RESEARCH INSTITUTE
2800 LYNGBY, DENMARK

Le Chef du Département GES — Le Directeur

C. BEGHIN — J. HIEBLOT

MARS 1981

RESUME

Sept pulses TBF, d'une durée de 1 seconde, émis à partir de l'émetteur Norvégien du système de navigation Oméga et observé à bord du satellite GEOS-1, sont analysés à partir de trois méthodes différentes de détermination de direction de normales d'ondes : le produit croisé d'échantillons successifs du vecteur champ magnétique de l'onde, la méthode de Means, et la méthode de détermination de la fonction de distribution des ondes basée sur le concept du maximum d'entropie. Les deux premières méthodes supposent que le champ électromagnétique est localement et instantanément celui d'une seule onde plane. La première est basée sur l'interprétation de la mesure des 3 composantes magnétiques du champ dans une bande de 300 Hz centrée sur la fréquence d'émission d'Oméga, la seconde sur l'interprétation de la matrice spectrale des 3 composantes magnétiques du champ à la fréquence d'Oméga. Dans la troisième méthode, le champ est supposé aléatoire. Il est caractérisé par une fonction de distribution des ondes (WDF) estimée à partir de la même matrice spectrale que celle utilisée dans la méthode de Means. On lève l'ambiguité sur la direction de $\vec{k}$ en ajoutant à la mesure des composantes magnétiques la mesure d'une composante électrique du champ. On compare et on discute les trois types de méthodes et leurs relations à partir des propriétés statistiques du signal : rapport signal sur bruit, stationarité en temps, degré de polarisation, valeur de la polarisation. En définitive, on trouve que les vecteurs $\vec{k}$ font un angle voisin de 140° avec la direction du champ magnétique terrestre et sont orientés légèrement à l'est du méridien magnétique local. Ils varient en fonction du temps avec une période de 0.2 à 0.4 seconde.

ABSTRACT

Seven VLF whistler-mode pulses of ~1 s duration, emitted from the Omega Navigation System transmitter located in Norway, and observed on-board the GEOS-1 satellite, are analysed by three different methods of determination of the wave normal directions : the cross-product of successive samples of the magnetic field vector, Means' method, and the Maximum Entropy Method of determination of the Wave Distribution Function. The two first methods assume that the electromagnetic field is locally and instantaneously like that of a single plane wave. The first is based on the interpretation of the 3 magnetic wave field components measurements in a 300 Hz band centered at the neighbourhood of the Omega frequency, the second on the interpretation of the spectral matrix elements of the 3 magnetic wave field components at the Omega frequency. In the third method the field is supposed to be random. It is characterized by a Wave Distribution Function (WDF) which is determined from the same spectral matrix as the Means method. Adding the measurement of one electric field component, one removes the ambiguity about the $\vec{k}$ direction. The three types of methods and their solutions are compared and discussed taking into account the statistical properties of the signal : Signal to noise ratio, stationarity in time, degree of polarization, polarization value. The $\vec{k}$ vectors are found to make angles of ~140° with the Earth magnetic field direction, and to point slightly Eastward of the local magnetic meridian. They admit a time variation of .2- to .4- sec periodicity.

1. INTRODUCTION

Numerous methods have been developped for determining the wave normal direction of the electromagnetic wave fields observed in space from the simultaneous measurement of part or all of the six wave field components. They can be classified in different ways depending on the importance which is attached on the hypothesis made on the wave (plane wave or not) or on the measured signals (deterministic or not). In practice, three types of methods can be distinguisted. In the type 1 method the wave is supposed to be plane and the signal deterministic. The wave normal direction is derived either from the computation of the cross-product $\vec{h}(t) \times \vec{h}(t + \tau)$, with $\vec{h}(t)$ the wave magnetic vector (Grard, 1968 ; Shawhan, 1970), or from an "instantaneous" complex representation of the signals (Kodera et al., 1977 ; Loisier et al., 1979). There is an ambiguity about the wave normal direction : longitudinal component in the $\vec{B}_o$ direction of the Earth magnetic field or in the opposite direction. It can be removed in the cross-product method if a minimum of 5 wave field components are measured. Such a capababity does not exist so far in the other method. In the type 2 methods the wave is supposed to be plane (Mc.Pherron et al., 1972 ; Means, 1972 ; Samson and Olson, 1980), or formed of a finite number of plane waves (Buchalet and Lefeuvre, 1981), but the signal is non-deterministic. The wave normal directions are determined by using the n x n spectral matrix of the n magnetic and electric wave field components ($n \leq 6$).
Mc Pherron et al. consider the eigenvector associated to the smallest eigenvalue of the Real part of the 3 x 3 spectral matrix of the magnetic components ; Means, the elements of the Imaginary part of the same 3 x 3 spectral matrix, Samson and Olson, the eigenvector associated to the highest eigenvalue of a n x n spectral matrix ($n \geq 3$) ; Buchalet and Lefeuvre, the full n x n spectral matrix ($n \geq 3$). The ambiguity about the wave normal direction can be removed in the two latter methods for $n \geq 4$. In the type 3 methods, the wave field is supposed to be random and the signal non-deterministic. The wave is characterized by a Wave Disribution Function (WDF) specifying, at a given frequency, how the energy is

distributed relatively to the wave normal direction (Storey, 1971) ; Storey and Lefeuvre, 1974, 1979). Techniques to derive the WDF from the estimation of a n x n spectral matrix are given in Lefeuvre, 1977 ; Lefeuvre and Delannoy, 1979, Lefeuvre et al., 1981. The ambiguity about the wave normal direction can be removed for $n \geq 4$.

Theoretically, all these methods give similar results in the pure plane wave case where one single wave normal direction can be associated to a set of given measurements (Lefeuvre, 1977). The point is to know how they behave in the quasi plane wave case, the only realistic case. Comparative studies on real data have already been published. However they concern methods of the same type (Arthur et al. 1976, and Samson and Olson, 1980 have compared type 2 methods between themselves) or methods of two different types (Buchalet and Lefeuvre, 1981 have compared one particular type 2 method and one particular type 3 method). Moreover insufficient attention has been given to the relationship between the statistical properties of the signal and the exact behavior of the different methods.

In the present paper we have taken the opportunity of the observation on-board the GEOS-1 satellite of 7 nearly successive pulses, of ~1 second duration, emitted at 10.2 and 11.33 kHz from the Omega Navigation System transmitter located in Norway, to compare one representative method of each type. The seven pulses are similar enough (quasi-plane wave) but also dissimilar enough (differences in intensity, stationarity, degree of polarization, polarization value) to lend credibility to our study. The three methods which have been chosen are : for type 1, the cross-product method (Shawhan, 1970), for type 2, the Means' method (Means, 1972), and for type 3 the Maximum entropy method (Lefeuvre and Delannoy, 1979). It is shown that the combination of several methods can be necessary to point out geophysical effects easily confused with estimation errors.

The plan of the paper is as follows. In section 2 the three methods are briefly reviewed. The experimental conditions and the statistical properties of the data are studied in section 3. Results of the different analysis are presented and discussed in section 4. Finally section 5 offers some conclusions.

2. THE METHODS

Notations

Through the whole paper the data are given in a satellite frame of reference while the results are interpreted in a physical coordinate system. The satellite frame of reference we consider has its oz axis along the spin axis of the satellite, and its ox and oy axes along the radial antennas. In the physical coordinate system, oz is parallel to the Earth magnetic field direction $\vec{B}_o$, ox is in the magnetic meridian plane containing the point of observation, and oy, completing the orthogonal set, is oriented eastwards. The wave normal $\vec{k}$ is characterized, in the physical coordinate system, by a polar angle θ and an azimuthal angle ϕ (Figure 1).

In the first system the axial components of the electric and magnetic field of the wave are respectively denoted e_x, e_y, e_z and h_x, h_y, h_z. From these variables a general electric vector ε, with six components, is defined as follows.

$$\varepsilon_{1,2,3} = e_{x,y,z} \quad ; \quad \varepsilon_{4,5,6} = z_o\, h_{x,y,z} \tag{1}$$

where z_o is the wave impedance of free space. Let ε_i be any component of this vector ($i = 1,\ldots,6$). Then, at a given frequency ω_o, the spectral matrix $S(\omega_o)$ is defined in such a way that each of its 36 elements $S_{ij}(\omega_o)$ is either the mean auto-power spectrum of the field component ε_i (if $i = j$), or the mean cross power spectrum of the components ε_i and ε_j (if i is not equal to j).

The method we use to estimate $S_{ij}(\omega_o)$ is based on time averaging over short modified periodograms (Welch, 1967). Let $\varepsilon_i(l)$ and $\varepsilon_j(l)$, ($l = 0,.. N-1$) be the samples of the components i and j, taken in the time interval T, in the frame of reference of the satellite. The records are sectionned in K segments, possibly overlapping, of length L ($l = 0, .. L-1$). We consider a Parzen window w(l) and, for each segment, form the sequence $\{\varepsilon_i(l)w(l)\}_k$,$\{\varepsilon_j(l)w(l)\}_k$. We

then take the finite Fourier transforms of these sequences, noted $A_k(n)$, $B_k(n)$ respectively, and obtain the K modified periodograms

$$I_K(\omega_n) = \frac{L}{U} \{A_k(n)\ B_k^*(n)\} \qquad (2)$$

with $\omega_n = 2\pi n\ L$ and $U = L^{-1} \sum_{l=0}^{L-1} W^2(l)$. The spectral estimate is the average of these periodograms. It is noted :

$$\hat{S}_{ij}(\omega_n) = \frac{1}{K} \sum_{k=1}^{K} I_k(\omega_n) \qquad (3)$$

Although the signals considered here are not band-limited white noise , we assume the estimates unbiassed. Their variance is of the order of $1/\sqrt{K'}$ with $K' \geq K$ the total number of segments overlapping included. For K' large enough we have a more accurate estimation taking for the variances : var $\{Re(\hat{S}_{ij})\}$ = var $\{Re(I_K)\}/K'$; var $\{Im(\hat{S}_{ij})\}$ = var $\{Im(I_K)\}/K'$, where Re and Im mean Real and Imaginary part.

For practical reasons it is sometimes necessary to distinguish the Real and Imaginary parts of S_{ij} (or $\hat{S}_{ij}$). We then consider the quantities P_k (or $\hat{P}_k$) with $P_1 = S_{11}$, $P_2 = Re(S_{12})$, $P_3 = Im(S_{12})$, ... $P_{36} = S_{66}$.

The cross-product method

The cross-product method is based on the following simple relation between the wave normal $\vec{k}$ and the wave magnetic field vector $\vec{h}$

$$\vec{k} \cdot \vec{h} = 0$$

To find the $\vec{k}$ direction one first defines the unit vector $\vec{n}$ normal to the polarization ellipse described by $\vec{h}$. It is given by the expression

$$\vec{n} = \frac{\vec{h}_{i+j} \times \vec{h}_i}{|\vec{h}_{i+j} \times \vec{h}_i|} \qquad (4)$$

where the samples $\vec{h}_i$ and $\vec{h}_{i+j}$ of the magnetic field vector are chosen in such a way that the angle $(\vec{h}_i, \vec{h}_{i+j})$ be as close as possible to 90°. This is illustrated in Figure 2 for the idealized case of a single monochromatic circularly polarized plane wave. As the wave propagates in the right hand polarized whistler mode, i.e. as the magnetic field rotates in the direction of the electrons, there is an ambiguity in the sign of the vector $\vec{k}$ which is either parallel or antiparallel to the unit vector $\vec{n}$. Such an ambiguity is easily removed in the case of the Omega signals where the energy obviously propagates from the Earth up to the satellite, which means, in the Northern hemisphere that the $\vec{k}$ vectors have their longitudinal components in the direction opposite to $\vec{B}_o$. From here and after we shall take $\vec{k} \equiv \vec{n}$, $\vec{k}$ being considered as a unique vector.

The signal being always more or less noisy, the polarization ellipse fluctuates making the estimation of the $\vec{k}$ vectors random. This is the reason why we have replaced the equation (4) by :

$$< \vec{k} > = \frac{\sum_{i=1}^{N} \vec{h}_{i+j} \times \vec{h}_i}{\left| \sum_{i=1}^{N} \vec{h}_{i+j} \times \vec{h}_i \right|} \qquad (4\text{-a})$$

In order to be able to detect time variations of the $< \vec{k} >$ vectors we have fixed N to 16 which corresponds to a time resolution of the order of 11 msec.

For comparisons with the Means and WDF solutions we have also been led to estimate an average of the $\vec{k}$ vectors over an interval time of 86 msec. (128 samples).

In both cases the Frequency resolution is of the order of 300 Hz which is the bandwith of the Swept Frequency Analyzer on GEOS (see section 3).

The Means method

In the Means method $\vec{n}$ is directly derived from the elements of the Imaginary part of the spectral matrix. It is written :

$$\vec{n} = \frac{1}{\Delta} \begin{bmatrix} \eta_x \\ \eta_y \\ \eta_z \end{bmatrix} \qquad (5)$$

with, in our notations, $\eta_x = \mathrm{Im}\{\hat{S}_{56}(\omega_o)\}$, $\eta_y = -\mathrm{Im}\{\hat{S}_{46}(\omega_o)\}$, $\eta_z = \mathrm{Im}\{\hat{S}_{45}(\omega_o)\}$, and $\Delta = |\vec{n}|$. In the physical frame of reference of Figure 1, we have :

$$|\cos\theta| = -\eta_z/\Delta \qquad (6)$$

$$\mathrm{tg}\phi = \eta_y/\eta_x \qquad (7)$$

Note that the method assumes that the wave has a circular or elliptical polarization. If the polarization is linear, what is theoretically impossible in the whistler mode case, we have a negative value for equation (6), which is obviously meaningless. As for the cross-product we shall assume that there is no sign ambiguity in the $\vec{k}$ direction for the Omega signals. Therefore we shall consider $\vec{k} \equiv \vec{n}$, with $\vec{k}$ unit vector.

The Maximum Entropy method of determination of the WDF

In this approach the electromagnetic field is considered as random. It is characterized by a Wave Distribution Function (WDF) which specifies, at a given frequency, and for a given mode of propagation, how the wave energy is distributed relatively to the wave normal direction $\vec{k}$. At the frequency ω_o it is noted $F(\omega_o, \cos\theta, \phi)$.

The WDF is related to the auto and cross-spectra of the wave field components by the equation :

$$S_{ij}(\omega_o) = \frac{\pi}{2} \oiint a_{ij}(\omega_o, \cos\theta, \phi) \; F(\omega_o, \cos\theta, \phi) \; d\sigma \qquad (8)$$

The kernels $a_{ij}(\omega_o, \cos\theta, \phi)$ are known analytical functions which implicitely depend on the parameters of the ambiant plasma ; here the electron gyrofrequency Ω_e and the electron plasma frequency Π_e (Storey and Lefeuvre, 1980). $d\sigma = d\cos\theta \, d\phi$ is the surface element. The integral is taken over the surface of the sphere of unit radius.

When deviding equation (8) in the Real and Imaginary part, one obtains a maximum of 36 equations of the type.

$$P_k(\omega_o) = \frac{\pi}{2} \oiint q_k(\omega_o, \cos\theta, \phi) \; F(\omega_o, \cos\theta, \phi) \; d\sigma \qquad (9)$$

with $q_1 = a_{11}$, $q_2 = Re(a_{12})$, $q_3 = Im(a_{12})$, ... $q_{36} = q_{66}$.

Except in the pure plane wave case, where $F(\omega_o, \cos\theta, \phi)$ is identical to a dirac distributions $\delta(\omega_o, \cos\theta - \cos\theta_o, \phi - \phi_o)$, the problem of determining $F(\omega_o, \cos\theta, \phi)$ from the measured values $\hat{P}_k$ of the P_k's is improperly posed in the sense that it admits infinitely many solutions. Among this infinity of solutions we choose the one which has the maximum entropy i.e. which maximize :

$$- \oiint F(\omega_o, \cos\theta, \phi) \; \text{Log} \; F(\omega_o, \cos\theta, \phi) \; d\sigma \qquad (10)$$

It has the expressions

$$F(\omega_o, \cos\theta, \phi) = \exp\{-1 + \sum_{k=1}^{M} \lambda_k q_k(\omega_o, \cos\theta, \phi)\} \qquad (11)$$

the unknown parameters λ_k being given values which minimizes a quantity of the form :

$$\Phi = \sum_{k=1}^{M} \frac{(\hat{P}_k - P_k)^2}{<\delta \hat{P}_k^2>} \qquad (12)$$

with $\hat{P}_k$ the measured data, P_k the model data and $<\delta \hat{P}_k^2>$ the variances in $\hat{P}_k$ (we assume the data are unbiassed and the errors on the data are uncorrelated).

Theoretically we have M = 36 for a 6 components measurement or more generally M = n x n for a n components measurement. However, to avoid numerical instabilities in the solution we are led only to consider the M "most" linearly independant q_k's. More details are found in Lefeuvre and Delannoy (1979) and in Lefeuvre et al. (1981).

The actual instability (distortion of the solution for a slight change in the data) is measured by the ratio between the mean-square error of the solution and the mean-square value of the solution itself. It is written :

$$Q = \frac{\oiint < \delta F^2(\omega_o, \cos\theta, \phi) > d\sigma}{\oiint F^2(\omega_o, \cos\theta, \phi)\, d\sigma} \qquad (13)$$

with (Lefeuvre and Delannoy, 1979) :

$$< \delta F^2(\omega_o, \cos\theta, \phi) > \simeq H^{-1} F^2(\omega_o, \cos\theta, \phi) \qquad (14)$$

the matrix H being an hessian matrix whose elements are given by : $H_{kL} = \partial\Phi/\partial\lambda_k \partial\lambda_L$. A solution is considered stable if $Q \leq 1$. However the threshold has only a physical meaning if the errors on the data are well estimated.

The discrepancy between the measured data and the predicted ones (reconstructed from the solution) is given by the quantity

$$P_r = \frac{1}{N} \sum_{k=1}^{N} \frac{(\hat{P}_k - \tilde{P}_k)^2}{< \delta \hat{P}_k^2 >} \qquad (15)$$

N means that we consider all the N available data (36 for a 6 components measurement). The data are correctly fitted for $P_r \simeq 1$.

3. THE DATA

Experimental conditions

The signals we are considering are transmitted by the Omega Navigation System transmitter located in northern Norway at 62° 25' 15'' N, 13° 09' 10'' E. They are excited as pulses of 0.9, 1.0 or 1.1 sec length at 10.2 kHz, 11.33 kHz or 13.6 kHz in a format shown in Figure 3 (Burhans, 1974). In the analysis we treat the 7 strongest pulses received on GEOS-1 on day 361, 1977 from 08.06 to 08.11 UT, 4 of which are on 10.2 kHz and 3 on 11.33 kHz.

For this particular experiment only 4 of the 6 wave fields components are properly measured, these are the 3 magnetic components and the E_y electric component measured with a 40 m long electric antenna. We use data from the Swept Frequency Analyzers (SFA) which may sweep in the frequency range 150 Hz - 77 kHz by steps of 300 Hz. Theoretically the band pass is of 300 Hz but intense signals can be seen at frequencies slightly lower or higher than the cut-off frequencies. For a detailed description of the wave experiment on GEOS see S-300 experimentors (1979).

At the time of the observations of the Omega pulses the magnetometer on GEOS was malfunctionning and we have been forced to use a model for the magnetic field of the Earth. Following Ungstrup et al. (1978) we have used the Kosik model (Kosik, 1978) to estimate the Earth magnetic field vector $\vec{B}_o$ at the point of observation. We believe this estimation is good because the data are recorded relatively close to the earth ($3 \leq L \leq 4$) and because the observations were made during a magnetically quiet period ($K_p \leq 3$ since 5 days). The error induced on the determination of the electron-gyrofrequency is probably negligible (we take Ω_e = 28 kHz). However we cannot avoid uncertainties in the direction of the $\vec{k}$ vectors in a system of reference related to the Earth magnetic field direction.

Because the plasma density experiment was in saturation we have also been led to estimate the electron plasma frequency Π_e. This has been done extrapolating the plasma frequency measurements just before saturation. The value derived 118 kHz, has been found consistent with refractive index and time delay calculations. The plasma frequency value does not affect the $\vec{k}$ vector estimation when only the magnetic components are considered. Oppositely it plays a major role when one tries to remove the ambiguity in the $\vec{k}$ direction by including electric measurements as it will be seen in the WDF analysis.

Amplitude

The amplitude at the output of the SFA's varies between 0.2 and 0.7 mγ, which is weak relative to the typical amplitude (5-50 mγ) of the plasmaspheric hiss recorded around 450 Hz at the same L value (Thorne et al., 1972), but is consistent with the amplitude received above the NKL transmitter (Cornilleau et al., 1979) when the transmitter-satellite geometry and the radiated power (~ 10 KW) is taken into account .

On Figure 4 are represented the total magnetic field received by the three magnetic antennas and the electric field received by the long electric boom antenna (LEY). The pulses are numbered 1-7 according to the time of reception, number 1 is then the first pulse received and number 7 the last. This notation is used through all the paper. As the transmitter format is repeated every 10 seconds we have chosen to display the pulses on a normalized time scale (0-10 seconds) beginning at the time when the start of the pulses are transmitted. A first arrow marks the time when the front of the pulses reach GEOS, a second the time where the signal would vanish if no prolongation took place, and a third the time where a spectral analysis shows that the signal disappear. As already pointed out by Ungstrup et al. (1980) the Omega pulses are modulated at 2-3 Hz and prolongated from 0.5 to 1 second.

Note that, for technical reasons, pulses 3 and 6, emitted at 11.33 kHz, are observed through the step number 37 (theoretical pass band : 11.108 - 11.408 kHz), while the pulse 1, emitted at the same frequency, is observed during the first 0.69 sec through the step number 37, then through the step number 38 (theoretical pass band : 11.404 - 11.704 kHz). As far as the 10.20 kHz other pulses are concerned, pulses 2 and 5 are seen through the step number 33 (theoretical pass-band : 9.923 - 10.223 kHz) and pulses 4 and 7 through the step number 34 (theoretical pass-band : 10.219 - 10.519 kHz).

For each pulse a signal to noise ratio have been estimated computing $S/N = 20 \text{ Log } (|\vec{h}_S| / |\vec{h}_N|)$ where $|\vec{h}_S|$ and $|\vec{h}_N|$ are respectively the average modulus of the magnetic field of the signal and the average value of the magnetic field of the noise, in the 300 Hz SFA bandwith. The results, slightly pessimistic, are listed table 1. The pulses 2, 3 and 4 are the only ones to be out of the noise. The ratio S/N is maximum for the pulse 4, which is the less modulated pulse.

Let us now consider the spectral characteristic of the pulses. When derived from a single FFT, with a frequency resolution of $\sim$ 1.45 Hz, the spectra of the Omega pulses appear as more or less pure line spectra, a few Hz wide, whose maxima, 6 to 40 db out of the noise, are centered at frequencies slightly higher than the emitting frequencies. The shift in frequency, due to a Doppler-effect, is of the order of 3 Hz for pulse 2, 4 Hz for pulses 4 and 7, 5 Hz for pulse 1, 6 Hz for pulse 5, and 7 Hz for pulses 3 and 6.

Now, to apply Means and WDF methods, a spectral analysis has been performed each 86 msec, taking L = 64 and k = 2. Spectral matrices are derived at the Fourier components ω_o where the auto-power spectra of the magnetic wave field components have their maximum i.e., according to a translation in frequency, at 11.330 kHz then 11.323 kHz for pulse 1, 10.215 kHz for pulse 2, 11.330 kHz for pulse 3 and 6, 10.209 kHz for pulses 4 and 7, and 10.192 kHz for pulse 5.

They are analyzed as such in the Means method where a good time resolution is wished, and after having been averaged over the whole duration time of the pulses (K = 20 to 28) in the WDF method where the hypothesis of stationarity is required. In both cases the frequency resolution is of 23.25 Hz.

Signal to noise ratios have been estimated computing $S/N = 10 \text{ Log } \{P(\omega_o)/ <P(\omega_i) >\}$ where $P(\omega_o)$ is the power of the signal and $<P(\omega_i)>$ the mean power of the noise. They are compared table 1 to the signal to noise ratios at the output of the SFA's. Although not exactly ranked in the same way, pulses 2, 3 and 4 are still the far most intense.

Stationarity in time

The stationarity in time required for the three methods is very different. There is practically no need of stationarity in time for the calculation of the cross-product solutions (4). A stationarity in time of $\simeq$ 11 msec is sufficient for deriving the averaged cross-product solutions (4-a). It has to be of the order of 86 msec for the Means solutions, and of the order of the pulse duration for the WDF solutions. In the following the stationarity has been assumed for time intervals inferior or equal to 86 msec, while they are tested for longer time scales.

Run and trend tests (Bendat and Piersol, 1971) have been applied at levels of significance greater or equal to 0.01 on the samples of the modules of the $\vec{h}$ vector. As obvious from Figure 4, no pulse has been found stationary in time over its whole period of observation.

The same tests applied on the traces of the spectral matrices of the I_k's (see equation 2) have been found positive at level of significance 0.01 for pulse 2, 4, 5 and 7, and even at level of significance 0.025 for pulses 5 and 7, which indicates that the spectra are less disturbed by the modulation than the waveforms. This makes possible the use of the Means and WDF methods on the whole observation time of those pulses.

Degree of polarization

By analogy with the procedure followed in optics for a two wave field component measurements (Born and Wolf, 1959) a degree of polarization can be defined for a three (or more) wave field components measurement (Samson, 1973). It has for instance for expression :

$$P^2 = \frac{1}{2\left(\sum_{i=1}^{3} \lambda_i\right)^2} \times \sum_{j,k=1}^{3} (\lambda_j - \lambda_k)^2 \qquad (16)$$

Here, λ_1, λ_2, λ_3 are the eigenvalues of the averaged spectral matrix of the magnetic wave field components ranked in decreasing order. When $P \simeq 1$, or $\lambda_1 >> \lambda_2, \lambda_3$, the wave field is considered to be completely polarized. It is that of a single plane wave. When $P = 1$ the wave field can be described by two plane waves if $\lambda_1, \lambda_2 >> \lambda_3$ and by three plane waves or more if $\lambda_1 \simeq \lambda_2 \simeq \lambda_3$ (Buchalet, 1979, Buchalet and Lefeuvre, 1981).

The degree of polarization derived for each pulse are given in table 3. The pulses 3 and 4, which have the highest degree of polarization, are expected to have polarization values very close to the theoretical ones, estimated from the Maxwell's equations under the plane wave hypothesis.

Note that, if a degree of polarization cannot be directly derived from the waveforms, we can also have an idea of the validity of the plane wave approximation comparing measured and theoretical polarization values :

Polarization value

The polarization value is defined as the ratio of the small to the large axis of the ellipse described by the $\vec{h}$ vector. In the system of reference where oz is parallel to $\vec{k}$ it is given by $R = (h_x/h_y)_{min}$ Here, according to the experimental wave and plasma parameters values, it is expected to have values between 0.95 (propagation close to the resonance cone of the whistler mode) and 1 (longitudinal propagation).

An attempt has been made to evaluate the R values each 86 msec. as shown on Figure 5 in the case of pulse 3. The polar diagram on the right represents the wave normal direction derived from equation (4-a) with N = 128 : the Earth magnetic field vector $\vec{B}_o$ is perpendicular to the paperplane, θ is the angle$(\vec{k}, \vec{B}_o)$ and ϕ an azimuthal angle (For $\phi = 0$, $\vec{k}$ is in the meridian plane ; for $\phi > 0$, $\vec{k}$ points Eastwards). The plot on the left shows an hodogram. The individual samples of the magnetic field vector of the wave are projected on a plane perpendicular to $\vec{k}$, the vertical axis is in the plane $\vec{k}$, $\vec{B}_o$, and the positive direction is away from the Earth (arbitrary scale).

A value of R can have been computed in 83 % of the interval time of 86 msec for pulse 4, 50 % for pulse 2, 42 % for pulses 1 and 3, 18 % for pulse 7, 7 % for pulse 6, and 0 % for pulse 5 ; the percentage of successful analysis being closely related to the signal to noise ratio at the output of the SFA s (see table 1). The mean values are listed table 4.

Now, the polarization can also be estimated from the Real part of the spectral matrix of the magnetic wave field components (Mc Pherron et al., 1972). If we note μ_1, μ_2, μ_3 the eigenvalues of this matrix, ranked in decreasing order, we have : $R'^2 = \mu_2 / \mu_1$; a R' value being always computable.

R' values have been estimated each 86 msec, then averaged. The results, summarized table 4, are surprising in many respects. First, they do not coincide with the results obtained from the waveforms. Second, they show polarization values much lower than expected. Third, they present cases of waves highly polarized but with a wrong polarization, this is especially obvious for pulse 3.

If the discrepancies between $< R >$ and $< R' >$ can eventually be attributed to the noise on the waveforms at the output of the SFA'S,

there is presently no simple explanation for the low polarization values, particularly in the cases of well polarized pulses. Is this due to the signal, to the SFA's, to the spectral analysis ? Two of the most circularly polarized pulses (pulses 4 and 7) and two of the most linearly polarized pulses (pulses 3 and 6) give arguments of equal values for each hypothesis. Pulses 4 and 7 are stationary in time while pulses 3 and 6 are not. Pulses 4 and 7 are the only ones to have a Doppler effect of 4 Hz while pulses 3 and 6 are the only ones to have a Doppler effect of 7 Hz. Pulses 4 and 7 are the only ones to be observed through the step number 37 of the SFA's while pulses 3 and 6 are the only ones to be observed through the step number 34. Pulses 4 and 7 are the only ones to be analyzed at a Fourier component 9 Hz above the emitting frequency while pulses 3 and 6 are the only ones to be analyzed at a Fourier component which exactly coincides with the emitting frequency.

What is granted is that, for waves with a high degree of polarization, a discrepancy between the experimental polarization value and the polarization value deduced from the Maxwell equations, is a proof of inconsistencies in the data.

4. THE RESULTS

The cross-product solution

Distribution functions of the individual wave normal directions derived from equation (4), assuming the $\vec{k}$ vectors oriented upwards, are plotted on Figure 6. The left plots are the distribution of $\cos\theta$ and the right plots the distribution of $\sin\phi$. The arrows on the figure indicate the position of the resonance cones : $\cos\theta_o$. The distributions are expected to be constant in $\cos\theta$ and to have a $1/|\cos\phi|$ dependance in ϕ if the processes are random and if the $\vec{k}$ vectors are uniformly distributed in θ and ϕ, without regards for the propagation condition in the whistler mode ($|\cos\theta| > |\cos\theta_o|$). Oppositely they are supposed to be well peaked in $\cos\theta$ as well as in $\sin\phi$ if the processes are deterministic and if the $\vec{k}$ vectors have constant values. From Figure 6 we establish that the pulses with low signal to noise ratio (pulses 1, 5, 6, 7) behave as random noise, while pulses with high signal to noise ratio (pulses 2, 3, 4) have a tendancy to behave like deterministic processes. At this step it is impossible to know if the dispersion around the peak values are only due to the noise in the 300 Hz band or to a time variation of the $\vec{k}$ vectors.

Wave normal directions seem to be better defined when derived from equation (4-a) with N = 16. The results are represented on Figure 7. The time axis is similar to that of Figure 4, i.e. it is normalized to 0 - 10 seconds. The top curve of each of the seven pulses is θ, the bottom curve ϕ and the dashed lines indicate the position of the resonance cone within which no wave can propagate and so the solutions have no physical meaning. The dispersion of the wave normal directions, on a time scale which is short relatively to the period of the wave amplitude modulation, closely follows the signal/noise ratios at the outputs of the SFA's. It is very weak for pulse 4, slightly emphasized for pulses 2 and 3, important for pulses 5 and 7, and especially strong for pulse 6, the last half of which being nearly indistinguishable from the noise. Oppositely the long time scale dispersion seems neither to relate to the signal/noise ratios nor to the polarization values. It is weak for pulse

4, 5 and 7, medium for pulse 3, and strong for pulse 1, 2 and 6. Considering only pulses 2, 3 and 4, where the signal to noise ratios make the wave analysis trustable, we clearly see that, over a long time scale, the wave normal directions have a time variation closely associated to the wave amplitude modulation.

The noise effect on a short time scale is easily understood adding noise vectors $\vec{\varepsilon}$ and $\vec{\varepsilon}'$ to the field vectors $\vec{h}_i$ and $\vec{h}_{i+j}$ in (4-a). Indeed, we define as a mean direction :

$$< \vec{k}_\varepsilon > = \frac{1}{\Delta} \{(\vec{h}_i \times \vec{h}_{i+j}) + (\vec{h}_i \times < \vec{\varepsilon}' >) - (\vec{h}_{i+j} \times < \vec{\varepsilon} >)\} \quad (17)$$

with Δ a normalization factor. The noise being supposed to have a gaussian distribution with zero-mean value and standard deviation σ, proportional to the signal/noise ratio : $< \vec{k}_\varepsilon >$ tends towards $< \vec{k} >$ when N is large enough (probably greater than 16) or when σ tends towards zero (high signal to noise ratio).

To facilitate the comparison with the other solutions, the $< \vec{k} >$ directions have been averaged over time intervals of 86 ms. The results are represented by circles on the θ, ϕ polar diagrams of Figure 8 and on the time varying diagrams of Figure 9. The time variation we have already pointed out for pulses 2, 3 and 4 seems to exist for all the pulses. This will be validated by the results obtained with the Means method.

The Means solutions

The Means method has been applied on interval time of 86 m sec. When they exist, the solutions are represented by crosses on Figures 8 and 9. If they are practically merged with the circles (the cross-product solutions) for pulses 4 and 7, they are often absent and far from the circles for all the other pulses. The ones which are within the resonance cone are meaningless.

The pulses 4 and 7 being the only ones to be nearly circularly polarized, the polarization value seems to be a key factor in the evaluation of the validity of the Means method. Probably because it

measures the quality of the spectral analysis. The signal to noise ratios and the degrees of polarization must have overpassed a certain threshold and so have no influence on the solutions.

Now, if the excellent agreement between the cross-product and the Means solutions is not very informative in the case of pulse 4, particularly intense, it is much more informative in the case of pulse 7 since it shows that, providing a correct average is made (see equation (4-a)), the cross-product method can be successfully applied even in the cases of negative signal to noise ratios. As a consequence, the time variation of the $< \vec{k} >$ vectors we observe on Figure 9 is not only physically meaningful for pulses 2, 3 and 4, but also for pulse 7, and probably for most of the others.

To estimate the uncertainty in the $\vec{k}$ directions, let us add an error vector $\vec{\varepsilon}$ to the $\vec{\eta}$ vectors of equation (5). The new direction has the expression :

$$\vec{k} = \frac{1}{\Delta'} \; (\vec{\eta} + \vec{\varepsilon}) \qquad (18)$$

with Δ' normalizing factor. The misalignement between $\vec{k}_\varepsilon$ and $\vec{k}$ is measured by the scalar product

$$\vec{k}.\vec{k}_\varepsilon = \frac{1}{|\vec{\eta}|\Delta'} \; \{|\vec{\eta}|^2 + \vec{\eta}.\vec{\varepsilon}\} \qquad (19)$$

Averaged values have been estimated by Parker (1980) randomly choosing the components of the $\vec{\varepsilon}$ vector from Gaussian distribution with zero mean values and standard deviations σ proportional to $\mathrm{Im}(\hat{S}_{ij})$. Here, for $\sigma < 70$ % (var $\{\mathrm{Im}(\hat{S}_{ij})\} < 1/\sqrt{K}$) one would obtain an average misalignement $\cos^{-1} < \vec{k}.\vec{k}_\varepsilon > \leq 48°$. However a much more important misalignement can occur when the $\vec{\varepsilon}$ components have not a zero mean value, which seems to be the cases particularly for pulses with wrong polarization values.

Note that it has been possible to estimate Means solutions from the averaged spectral matrices (time resolution 0.8 to 1.2 sec) for pulses 4 ($\theta \simeq 127°$, $\phi \simeq 22°$) and 7 ($\theta \simeq 121°$, $\phi \simeq 19°$) only. For the other pulses the solutions were meaningless ($|\cos\theta| < 0$ or $< |\cos\theta_o|$).

The WDF solutions

Let us first consider the analysises from the averaged spectral matrices of the magnetic field components only. Contours of the upward parts of the WDF are plotted on Figure 8 while the stability parameters (13) and the prediction parameters (15) are given in table 5. The θ and ϕ values of the peaks are indicated on Figure 9.

The agreement with the cross-product and Means solutions is almost perfect for pulses 4 and 7, which ones, as a matter of fact, have the best quality parameters. This confirms the validity of the WDF concept even in cases of nearly pure plane waves. The fit with the data, which we cannot check in the other methods, is obviously not perfect. The polarization values for the two pulses are of the order of 0.6 while the polarization values of the data reconstructed from the solutions are of the order 0.9 (0.99 for pulse 4 and 0.94 for pulse 7), and this, in spite of the dispersion in θ and ϕ of the distribution functions.

Once more the role played by the polarization value for the methods based on the interpretation of the spectral matrix is pointed out. The stationarity parameter which would be a key factor in the WDF analysis is nothing but a supplementary factor participating to the conditionning of the spectral matrix and so to the polarization value . As far as the degree of polarization is concerned it may explain the wide dispersion of the WDF in case of pulse 7.

The uncertainties in the WDF determination do not alone explain the disagreement between the three types of solutions for the other pulses, particularly in ϕ. However they exist and need to be explained very carefully.

Let us first consider the uncertainties due to the method itself without paying regards to the experimental errors in the data. When doing so we assume the Omega signal is a pure plane wave whose the frequency is 10.2 kHz and the WDF is a dirac distribution centered at $\theta = 130°$, $\phi = 20°$. Substituting this WDF into equation

(8), and taking for values of the plasma parameters the experimental ones, we can estimate a spectral matrix. The only errors we make on the simulated data are numerical. We assume they are of the order of 10 %. The WDF derived from the maximum entropy method is represented on Figure 10. Considering the half width of the solutions, at half the maximum value, we see that the method induces a dispersion of the order of 7° in θ and 11° in ϕ. According to the high degree of polarization of most pulses, the wider dispersion of the WDF's we observe on Figure 8 seems to be due to the errors in the data.

Let us now consider the effect of the errors in the data. In a first approximation, we can consider that the perturbations $\delta F(\omega_o, \cos\theta, \phi)$ they induce on the WDF have zero mean values and are characterized, at each point θ, ϕ, by the standard deviation $< \delta F^2(\omega_o, \cos\theta, \phi) >$ calculated in (14). As an example we have plotted on Figure 11 cross-sections through the peak, of the WDF of pulse 4 ; the standard deviation being represented by error bars. We see that, if the uncertainties caused on the peak determination of the WDF by the errors in the data are often negligeable in θ relatively to the uncertainties due to the method ; they may be very important in ϕ, which is normal if we consider the smooth variation of the a_{ij} s in ϕ (Storey and Lefeuvre, 1980).

Very particular shifts in ϕ, such as the one of pulse 6, can be explained otherwise. Looking at the algebraic expressions of the a_{ij} s in the whistler mode (Lefeuvre, 1977 ; Storey and Lefeuvre, 1980) one finds that, in presence of noise, or of any inconsistencies in the data, it is very easy to make the confusion between the spectral matrices of waves whose $\vec{k}$ vectors have azimutal angles respectively at $\pi/8$ and at $\pi/8 + 3\pi/4$. In the frame of reference of Figure 1, for instance, they only differ by the sign of $Re(\hat{S}_{45})$, $Re(\hat{S}_{46})$ and $Im(\hat{S}_{56})$. It is likely that other couples of that sort exist for other θ and ϕ values. One is recommended to test for this if there are some reasons to question the validity of the WDF ; i.e. for instance, if the solution is strongly modified when the number of items of information used for the analysis is increased from 6 to 8, which is the case here for pulses 3 and 6

known to have very inconsistent data. Note that the Means method, based on the interpretation of the 3 Imaginary part of the cross-spectra only, is still more sensitive to this phenomenon. This explains the dispersion in ϕ of the crosses particularly for the pulses 1 and 2.

Now, oppositely to the others, the WDF approach theoretically allows to remove the ambiguity about the $\vec{k}$ direction (longitudinal component in the $\vec{B}_o$ direction or in the opposite direction) when one adds the electric component measurement E_y to the magnetic ones. However, such an operation can only be done for good quality measurements, which is not always the case for the Omega pulses; Nevertheless we show on Figure 12 that the maximum entropy method enables us to completely remove the $\vec{k}$ ambiguity for pulse 4. The shift in ϕ between the solutions of Figure 8-d and 12 is not that surprising if we remember that, due to the uncertainty on the plasma frequency value and to the imperfect estimation of the coupling impedance between the plasma and the sphere of the antennas, the errors on the electric measurements are much more important than the errors on the magnetic ones. As far as the other pulses are concerned, the ambiguity is partially removed for pulses 7, 1 and 2, in the sense that there is a residual image of the symmetric part of the solution,and not at all for pulses 3, 5 and 6.

6. CONCLUSION

We have applied three different methods of determining the wave normal directions of whistler mode pulses emitted by the Omega Navigation System transmitter in Norway and received on the GEOS-1 satellite. The three methods are the cross-product method, Means method, and the maximum entropy method of determination of the Wave Distribution Function (WDF). The methods and their results have been discussed in the context of statistical parameters : signal to noise ratio, stationarity, degree of polarization, and polarization value.

The signals being of the plane wave type, it has been found that the key parameter for the application of the cross-product method was the signal to noise ratio. Solutions are fully trustable for positive signal to noise ratio (signal > noise) but need agreement with solutions obtained from an alternative method to be validated for negative signal to noise ratio.

In the same way, the waves being highly polarized, the key parameter found for the two other methods, based on the interpretation of a spectral matrix, is the polarization value deduced from this spectral matrix. A discrepancy between the experimental polarization value and the polarization value derived from the Maxwell equations is indeed an indicator of inconsistencies in the data. Such inconsistencies affect first the Means method which only uses three items of information assuming they are without errors. But, when they are too important they can also make the WDF solutions untrustable . The signal to noise ratios having overpassed a certain threshold have not interfered in the analysis. The stationarity appeared in an indirect way contributing to the conditionning of the spectral matrix and so to the polarization values.

One conclusion of this comparative study is that the three methods are not too sensitive to the hypothesis made on the wave. The plane wave approximation can be used even for beams slightly dispersed in $\vec{k}$ vectors. In the same way a random approach can be adopted even for a quasi-plane wave. The hypothesis about the measured signal is a little bit more compulsory. As it has been shown with the cross-product solutions it is difficult to follow a completely deterministic approach. Wave normal solutions are generally meaningful only after having been averaged.

Now, to avoid useless computations and to try to obtain the most accurate solution in any situation, it is recommended to respect the following principles.

(1) - the spectral analysis being always subject to estimation errors, methods based on the interpretation of the spectral matrix have to be used when absolutely necessary only.

(2) - as a consequence of (1), if there is some reason to believe that the electromagnetic field is of the plane wave type, and if the signal to noise ratio estimated from the waveforms of the field components is high enough, type 1 methods must be applied. The validity of the plane wave hypothesis can be checked comparing for instance the ratio $(h_x/h_y)_{min}$ of the measured magnetic field components, taken in the system of coordinates with oz parallel to $\vec{k}$, to the theoretical polarization values calculated from the Maxwell equations. For medium and low signal to noise ratio, the type 1 method is still preferred provided that the signal is stationary enough to allow the computation of a physically meaningfull averaged $\vec{k}$ vector. However it must be remembered that the type 1 methods which allow to remove the ambiguity about the $\vec{k}$ direction (Grard, 1968 ; Shawhan, 1970) need the measurement of 5 wave field components at least.

(3) - when the waveforms are noisy or/and the plane wave hypothesis is questionable, it is better to work with spectral matrices ; the quality of the estimated spectra depending on the stationarity of the signals and on their signal to noise ratios. Then it is recommended to start the analysis by a calculations of the eigenvalues of the spectral matrices (at least of the 3 x 3 spectral matrices

of the magnetic wave field components). When a single non-zero eigenvalue is found, or which is the same, when a high degree of polarization is found , one gains computation time using a type 2 method based on the plane wave approximation. The quality of the data can even be tested prior any wave normal determination, comparing the polarization value derived from the measured spectral matrix to the theoretical value allowed by the Maxwell equations. The ambiguity about the $\vec{k}$ direction can be removed using the Buchalet and Lefeuvre's method when a minimum of four wave field components are measured.

(4) - for a low degree of polarization, two cases can be distinguished. First, if there are two non-zero eigenvalues only, the wave field can be described by the means of a two plane wave model, and the Buchalet and Lefeuvre's method must be chosen. Second, if the three eigenvalues have value of the same order, the WDF approach is the only possible one. In the latter case the quality of the estimation (and the quality of the estimated data) is a posteriori checked looking at the stability and prediction parameters. In both cases the ambiguity about the $\vec{k}$ direction can be removed if a minimum of four wave field components are measured.

From a geophysical point of view, the three methods used in the paper show that the Omega pulses propagate with oblique wave normals ($\theta \simeq 130°-140°$) pointing slightly Eastwards off the local magnetic meridian ($\phi \simeq 20°$), which is consistent with the observations made from the FR-1 satellite, at 750 km altitude, in the near zone of the Sainte-Assise transmitter, using the Grard's (1961) method (Aubry, 1968 ; Cairo and Cerisier, 1976). The WDF analysis , applied on one electric and three magnetic wave field components measurements enables us to check that the waves propagate upwards, with their wave normal direction in the direction opposite to the Earth magnetic field direction. The cross-product method, occasionally validated by the Means method, points out a time variation of the wave normal directions with a 0.2- to 0.4- sec. periodicity. Whether this variations is related to the modulation and the prolongation of the pulses will be the subject of a separate publication.

Pulse	SFA	Spectra
1	- 3.5 db	12.5 db
2	2.5 db	16.3 db
3	1.0 db	14.8 db
4	6.8 db	13.7 db
5	- 5.2 db	10.1 db
6	-12.2 db	8.9 db
7	- 6.4 db	8.2 db

Table 1

Averaged signal to noise ratio computed from the waveforms (second column) and from the spectra (third column).

Pulse	Run test	Trend test
1	*	-
2	+	*
3	*	-
4	*	+
5	*	*
6	-	-
7	*	*

Table 2

Stationarity in time of the spectra. The stationarity hypothesis is tested from run and trend tests at the levels of significance 0.01 and 0.025. The symbol - means that the hypothesis is rejected, + that the hypothesis is accepted at the 0.01 level of significance, and * that it is accepted at the level 0.025.

Pulse	λ_1	λ_2	λ_3	P
1	293.	20.	4.	0.887
2	443.	52.	5.	0.833
3	475.	13.	5.	0.945
4	1002.	10.	4.	0.979
5	120.	8.	4.	0.864
6	102.	10.	4.	0.820
7	125.	8.	4.	0.869

Table 3

Degree of polarization. λ_1, λ_2, λ_3, are the eigenvalues (in arbitrary units) of the averaged spectral matrices at ω_o. P is the degree of polarization defined in (16).

Pulse	< R >	< R' >
1	.8	.5
2	.7 +	.4
3	.8	.2
4	.8 *	.6
5	?	.3
6	.8	.3
7	.9	.6

Table 4

Polarization values. Averages are made from polarization values estimated each 86 msec from the waveform (R) and from the spectra (R'). In column 2, the symbol * means that a R value was computable in at least 75 % of the time and the symbol + in at least 50 % of the time . For pulse 5 no R value could be derived. In column 3 a R' value was always computable.

	Q	P_r
1	2.17	6.34
2	1.37	8.14
3	0.64	23.31
4	0.65	4.75
5	1.52	8.62
6	0.87	7.80
7	0.76	3.48

Table 5

Stability and Prediction parameters for the WDF derived using 7 of the 9 items of information available in the analysis of the 3 magnetic wave field components.

FIGURE CAPTIONS

Figure 1 : The physical coordinate system. The oz axis is parallel to the magnetic field of the Earth, ox is in the meridian plane containing the point of observation and oy is oriented eastwards.

Figure 2 : Determination of the wave normal direction by the cross-product method ($\vec{k}.\vec{h} = 0$).

Figure 3 : Time sequence of the 10.2 kHz, 11.33 kHz and 13.6 kHz transmissions from the Omega Navigation System transmitter in 1977 (Burhans, 1974) start time was 4 sec, 14 sec, etc. past the minute.

Figure 4 : Seven Omega pulses received on GEOS-1 day 361, 1977 from 08.04 - 08.11 UT. The pulses are numbered according to the time of reception. The top curve of each plot shows the modulus of the magnetic field and the bottom curve the signal on the large electric boom antenna (LEY). The time scale is normalized and start time of the plots is the start time of transmission of the pulses.

Figure 5 : Cross-product analysis of 86 msec of pulse 3. On the right : polar representations of the wave normal direction obtained from (4-a) using N = 128. On the left : hodogram of the magnetic field vector in the plane perpendicular to k ; the vertical axis is in the plane $\vec{k}$, $\vec{B}_o$, the positive direction being oriented away from the Earth, the scale is arbitrary.

Figure 6 : Distribution of the wavenormal direction calculated from (4). The arrows indicate the position of the resonance cone. 1280-1792 samples on each plot depending on pulse length.

Figure 7 : Wave normal directions calculated from (4-a) with N =16. The top curves represent the angle to the magnetic field of the Earth $\vec{B}_o$ and the bottom curves the azimuth angle positive eastwards of the meridian plane. The dashed lines indicate the position of the resonance cone.

Figure 8 : Distribution of the wave normals in a polar diagram centered on $\vec{B}_o$. The $\vec{k}$ vectors are assumed to be in the direction opposite to $\vec{B}_o$. The small circles represent the cross-product solutions averaged over 86 ms ; the crosses, the Means solutions estimated over the same time interval ; the full lines (see text) contours of the WDF's determined for the whole pulses. The inner circle, around 72° indicates the position of the resonance cone.

Figure 9 : Time variations of the θ and ϕ values estimated by the three methods. The cross-product solutions are represented by circles, the Mean solutions by crosses and the peak of the WDF by straight lines.

Figure 10 : Contours of the WDF for data simulated from a dirac distribution centered at $\theta = 130°$, $\phi = 20°$ (N = 9, M = 7, Q = 0.55, $P_r = 0.94$).

Figure 11 : Cross sections through the peak of the WDF of pulse 4 (see text).

Figure 12 : Contours of the WDF obtained for pulse 4 : (a) from the 3 magnetic components (Q = 0.65, $P_r = 4.75$) ; (b) from the 3 magnetic + the E_y components (Q = 0.92, $P_r = 10.22$).

REFERENCES

ARTHUR, C.W., R.L. MC. PHERRON, and J.D. MEANS, A comparative study of three techniques for using the spectral matrix in wave analysis, Radio Sci., 11, 833, 1976.

AUBRY, M., Influence des irrégularités de densité électronique sur la propagation des ondes TBF dans l'ionosphère, Ann. de Géophys., 24, 39, 1968.

BENDAT, J.S., and A.G. PIERSOL, Measurement and analysis of random data, pp 156-159, JOHN WILEY & SONS, New-York, 1968.

BORN, M., and E. WOLF, Principles of Optics, pp 544-550, Pergamon Press, Oxford, 1970.

BUCHALET, L.J., and F. LEFEUVRE, One-and two-direction models for VLF electromagnetic waves observed on board GEOS-1, J. Geophys. Res., to be published.

BURHANS, R.W., Phase-difference method offers low-cost navigation receivers, Electronics, 47, 98, 1974.

CAIRO, L., and J.C. CERISIER, Experimental study of ionospheric electron density gradients and their effect on VLF propagation, J. Atmos. terr. Phys., 38, 27, 1976.

CORNILLEAU-WEHRLIN N., R. GENDRIN, and R. PEREZ, Receptions of the NKL (JIM CREEK) transmitter on board GEOS-1, Space Sci. Rev., 22, 123, 1978.

GRARD, R., Interprétation de mesures de champs électromagnétiques TBF dans la magnétosphère, Ann. Géophys., 24, 995, 1968.

KODERA, K, R. GENDRIN and C. de VILLEDARY, Complex representation of a polarized signal and application of the analysis of ULF waves, J. Geophys. Res., 82, 1245, 1977.

KOSIK, J.C., The uses of past and present magnetospheric field models for mapping fluxes and calculating conjugate points, Space Sci. Rev., 22, 161, 1978.

LEFEUVRE, F, Analyse de champs d'ondes électromagnétiques aléatoires observés dans la magnétosphère à partir de la mesure simultanée de leurs six composantes, thèse de doctorat d'état, Université of ORLEANS, ORLEANS, FRANCE, 1977.

LEFEUVRE, F. and C. DELANNOY, Analysis of a random electromagnetic wave field by a maximum entropy method, Ann. Telecomm., 34, 204, 1979.

LEFEUVRE, F, M. PARROT, and C. DELANNOY, Wave Distribution Functions estimation of VLF electromagnetic waves observed on board GEOS-1, J. Geophys. Res., to be published.

LOISIER, G., N. CORNILLEAU-WEHRLIN, and R. GENDRIN, Normale d'ondes de signaux variant dans le temps, Ann. Telecomm., 34, 214, 1979.

MC PHERRON, R.L., C.T. RUSSEL, and P.J. COLEMAN, Fluctuating magnetic field in the magnetosphere, 2, ULF waves, Space Sci. Rev., 13, 411, 1972.

MEANS, J.D., The use of the three-dimensional covariance matrix in analyzing the properties of plane waves, J. Geophys. Res., 27, 5551, 1972.

PARKER, G.D., Propagation directions of hydromagnetic waves in interplanetary space : Pioneer 10 and 11, J. Geophys. Res., 85, 4283, 1980.

SAMSON, J.C., Descriptions of the polarization states of vector processes : application to ULF magnetic fields, Geophys. J.R. astr. Soc., 34, 403, 1973.

SAMSON, J.C., and J.V. OLSON, Some comments on the description of the polarization-states of waves, Geophys. J.R. astr. Soc., 61, 115, 1980.

SHAWHAN, S.D., The use of multiple receivers to measure the wave characteristics of very-low frequency noise in space, Space Sci. Rev., 10, 689, 1970.

STOREY, L.R.O., Electric field experiments : Alternating-fields in the ESRO Geostationary Magnetospheric satellite, Rep. SP-60, pp 267-279, European Research Organization, Neuilly-sur-Seine, FRANCE, 1971.

STOREY, L.R.O., and F. LEFEUVRE, Theory for the interpretation of measurements of a random electromagnetic waves field in space, Space Res., 15, 381, 1974.

STOREY, L.R.O., and F. LEFEUVRE, Analysis of a wave field in a magnetoplasma, 1, the direct problem, Geophys. J.R. Astron. Soc., 56, 255, 1979.

STOREY, L.R.O., and F. LEFEUVRE, Analysis of a wave field in a magnetoplasma, 2, the integration kernels, Geophys. J.R. Astron. Soc., 62, 173, 1980.

S-300 Experimenters, Measurements of electric and magnetic wave fields and of cold plasma parameter on board GEOS-1, Preliminary results, Planet. Space Sci., 27, 317, 1979.

THORNE, R.M., J.S. SMITH, R.K. BURTON, and R.E. HOLZER, Plasmaspheric hiss, J. Geophys. Res., 78, 1581, 1973.

UNGSTRUP, E., T. NEUBERT, and A. BAHNSEN, Observation on GEOS-1 of 10.2 to 13.6 kHz ground based transmitter signals, Space Sci. Rev., 22, 453, 1978.

UNGSTRUP, E., T. NEUBERT, and A. BAHNSEN, magnetospheric modification of Ground-based transmitter signals observed on GEOS-1, First International Symposium IMS results, La Trobe University, Melbourne, Australia, dec. 1979.

WELCH, P.D., The use of fast fourier transform for the estimation of power spectra : a method based on time averaging over short, modified periodograms, IEEE Trans. Audio and Electroacoust., 15, 70, 1967.

ACKNOWLEDGMENT

The authors express their gratitude to E. UNGSTRUP who initiated the GEOS-1 Omega experiment, to A. BAHNSEN for usefull discussions and to H. JAKOBSEN for helpful assistance in the data treatment. Thanks are also due to C. CHUDY for preparation of the final typescript. The work was supported by the Danish Natural Science Research Council and the "Centre National de la Recherche Scientifique" (France). Part of the study was done during a visit of one of us (F.L) to the Radio Science Laboratory, Standford University, thanks to a NSF-CNRS fellowship.

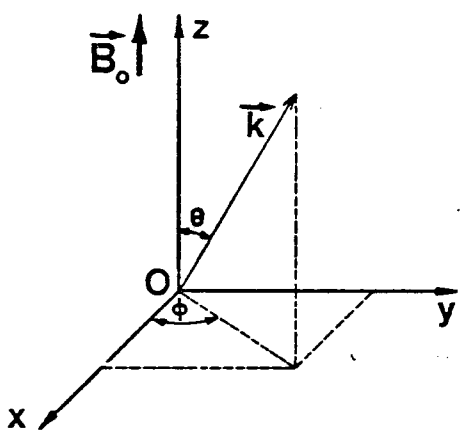

FIG.1

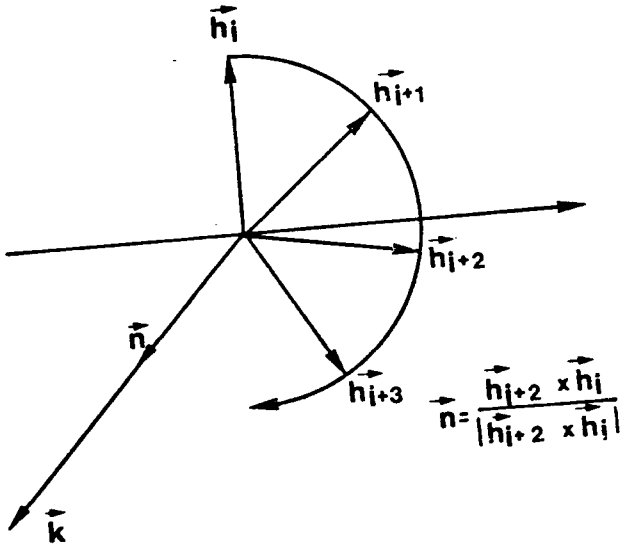
$\vec{h}_j$
$\vec{h}_{j+1}$
$\vec{h}_{j+2}$
$\vec{h}_{j+3}$
$\vec{n}$
$\vec{k}$
$\vec{n} = \frac{\vec{h}_{j+2} \times \vec{h}_j}{|\vec{h}_{j+2} \times \vec{h}_j|}$

FIG. 2

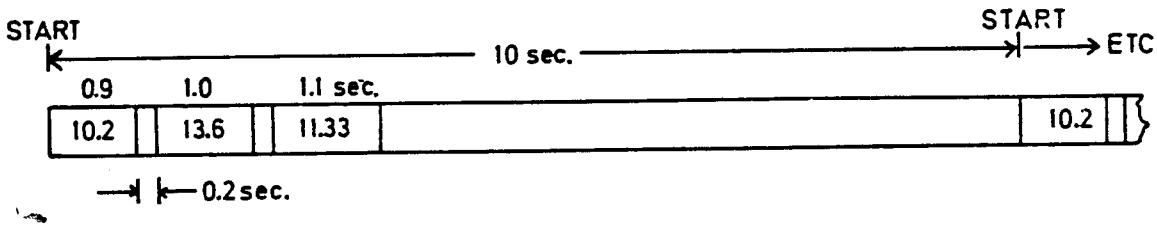

FIG.3

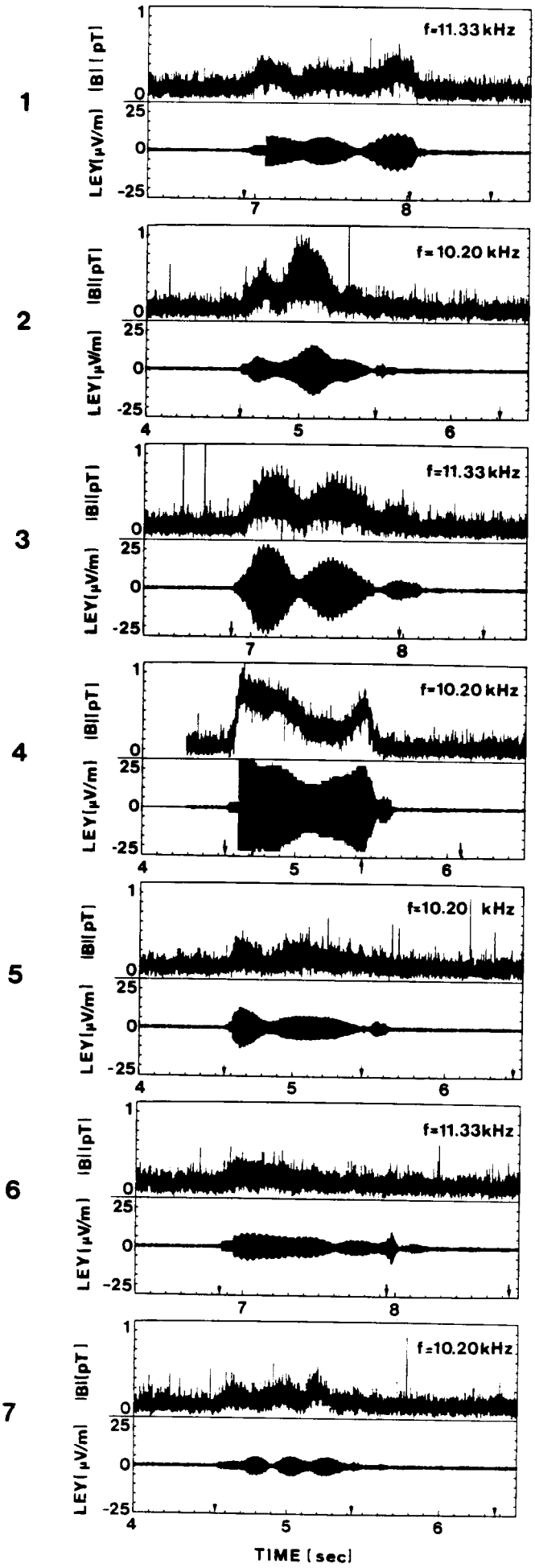
1
f=11.33kHz
|B| [pT]
LEY[μV/m]
2
f=10.20 kHz
|B|[pT]
LEY[μV/m]
3
f=11.33kHz
|B|[pT]
LEY[μV/m]
4
f=10.20 kHz
|B|[pT]
LEY[μV/m]
5
f=10.20 kHz
|B|[pT]
LEY[μV/m]
6
f=11.33kHz
|B|[pT]
LEY[μV/m]
7
f=10.20kHz
|B|[pT]
LEY[μV/m]
TIME [sec]

FIG.4

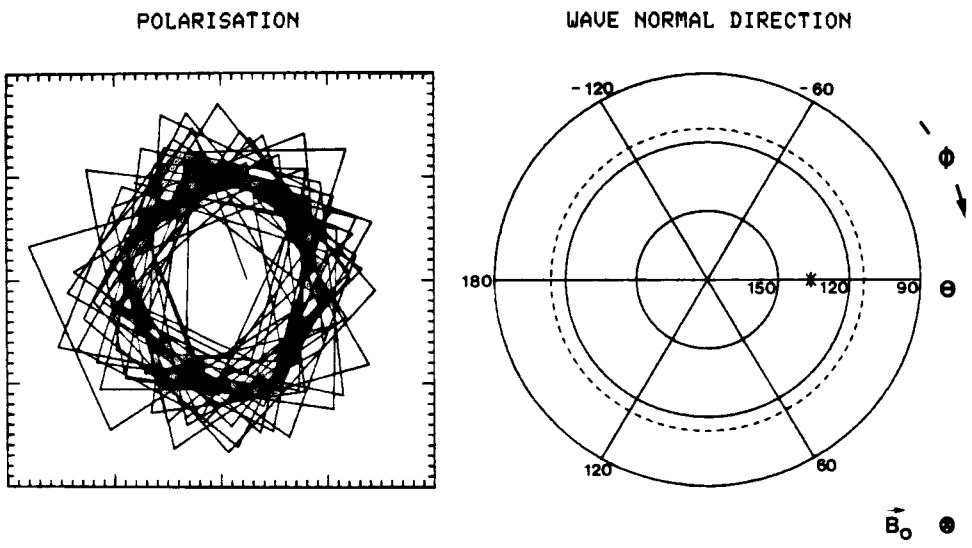
POLARISATION
WAVE NORMAL DIRECTION
-120
-60
180
150
120
90
120
60
Φ
Θ
$\vec{B}_o$

FIG.5

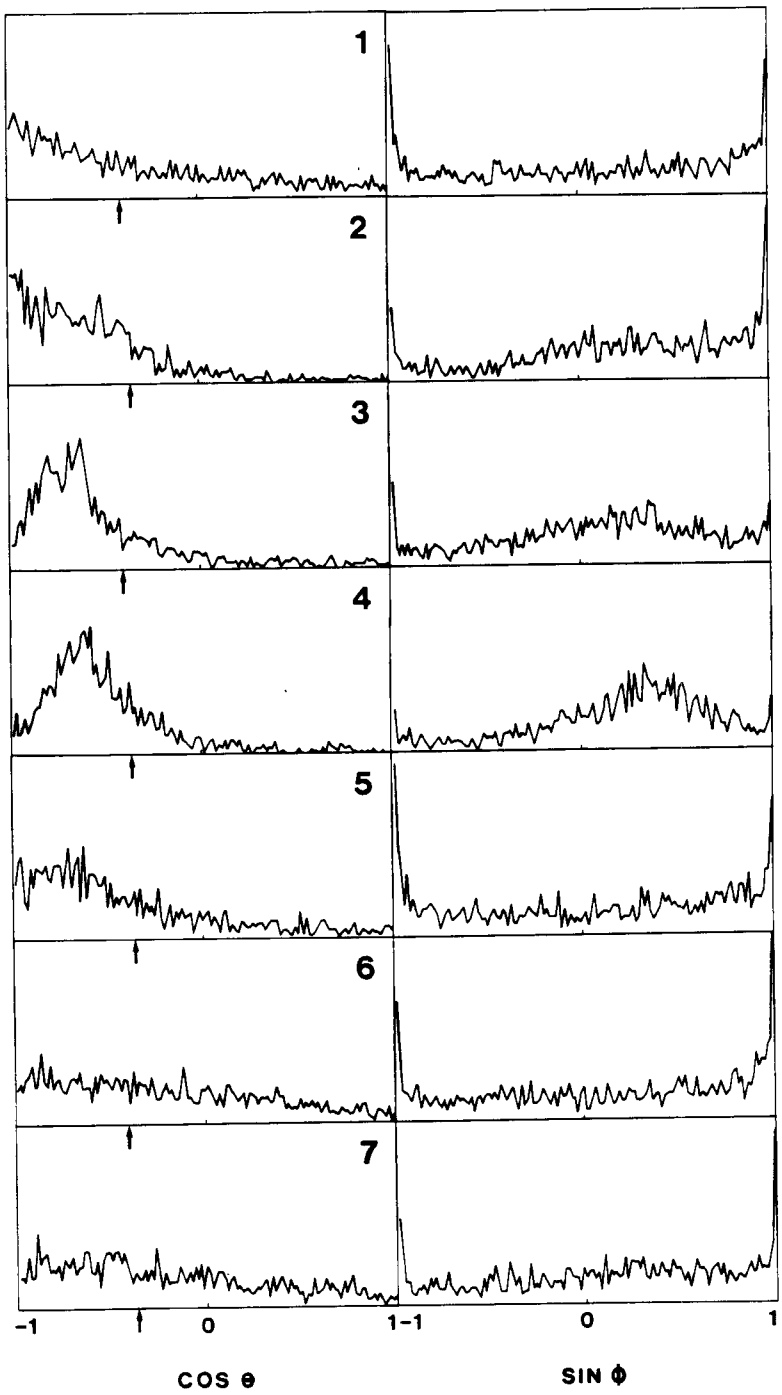

FIG.6

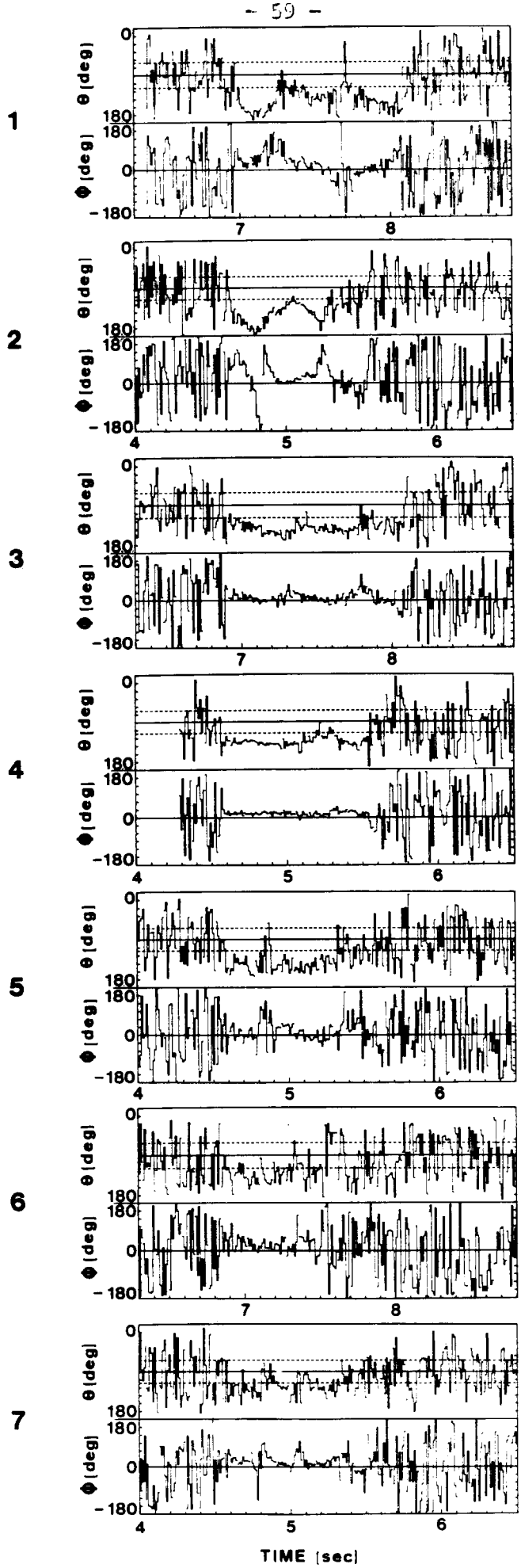

FIG.7

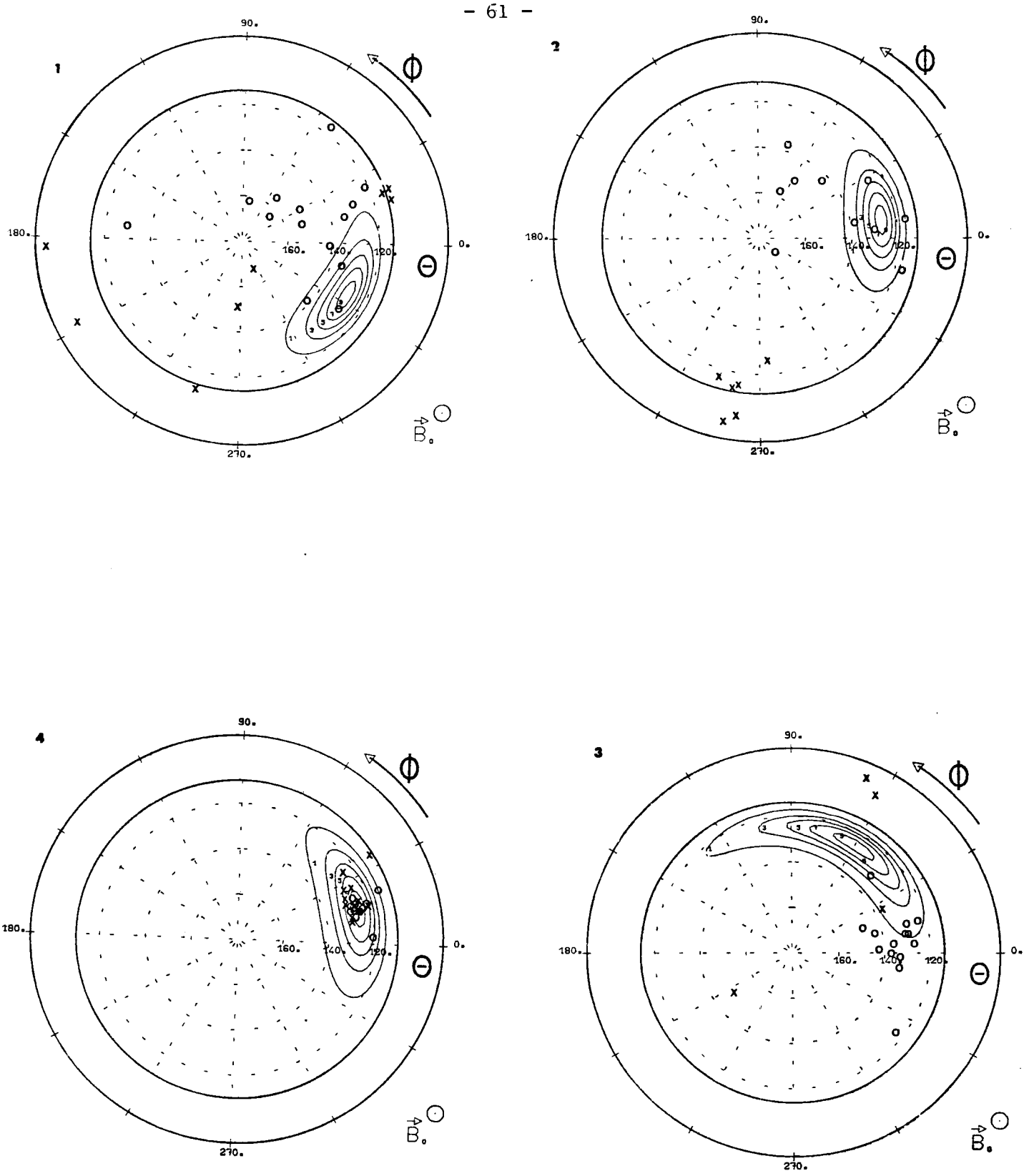

FIG.8

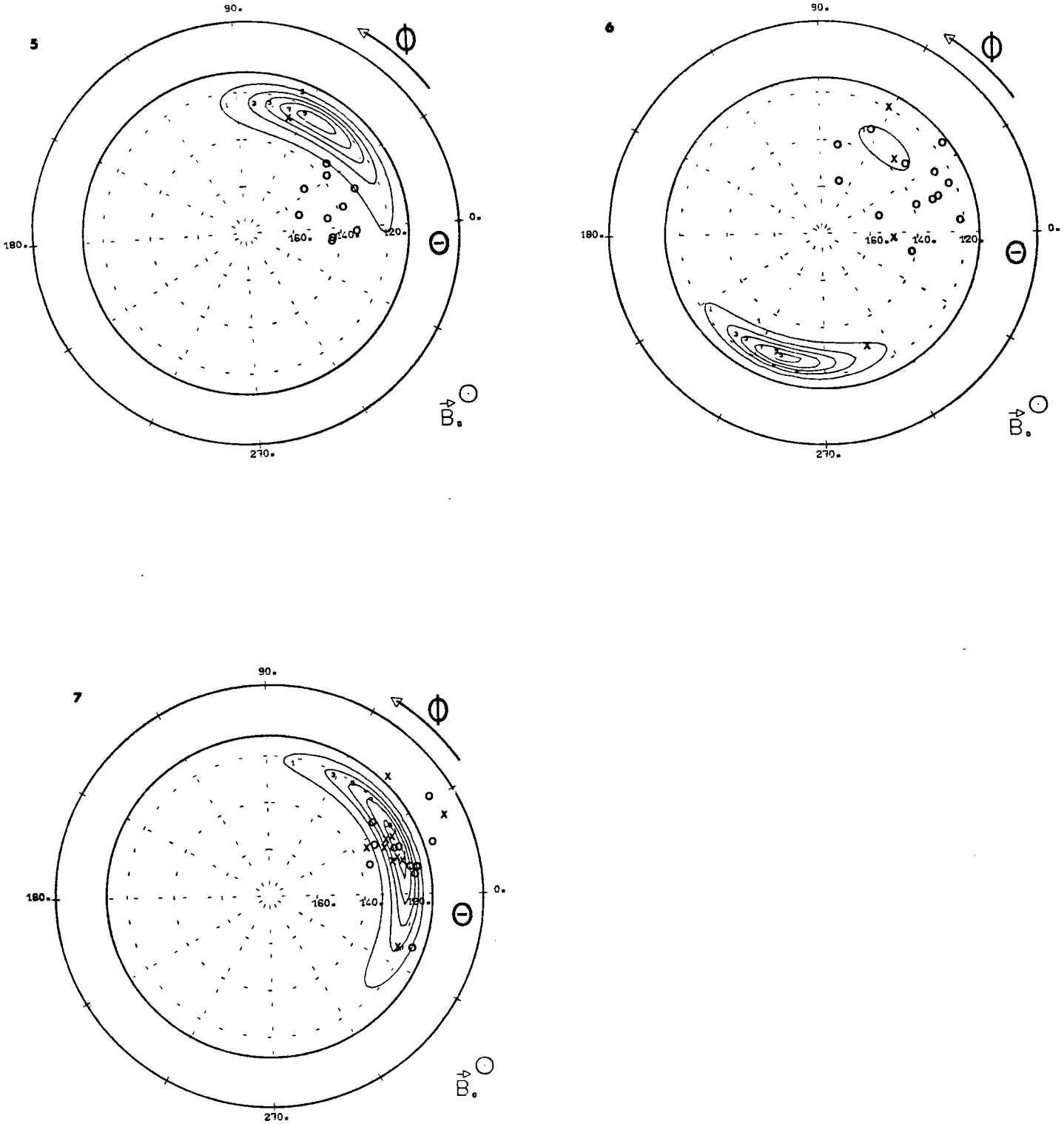

FIG.8

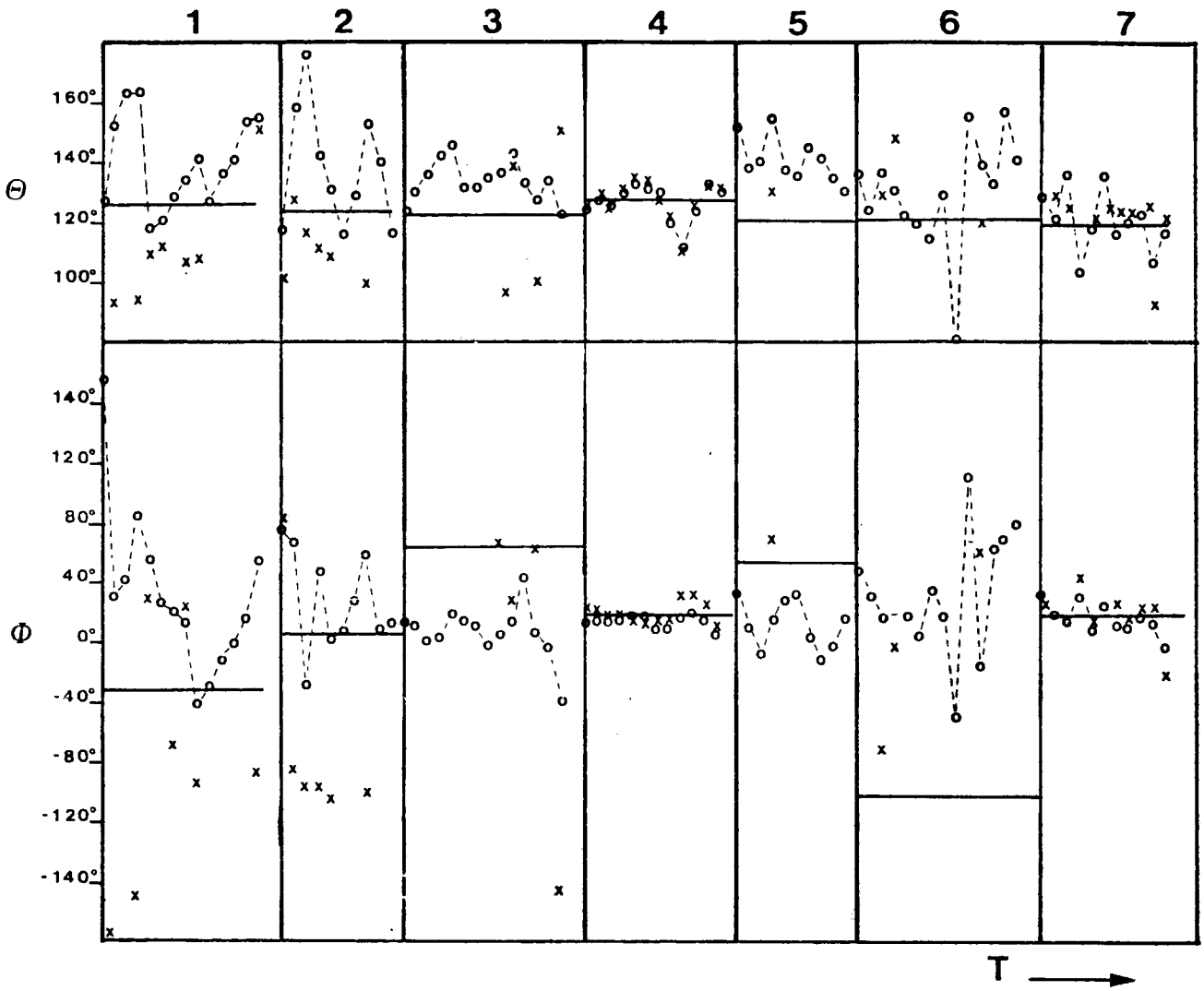

FIG. 9

c

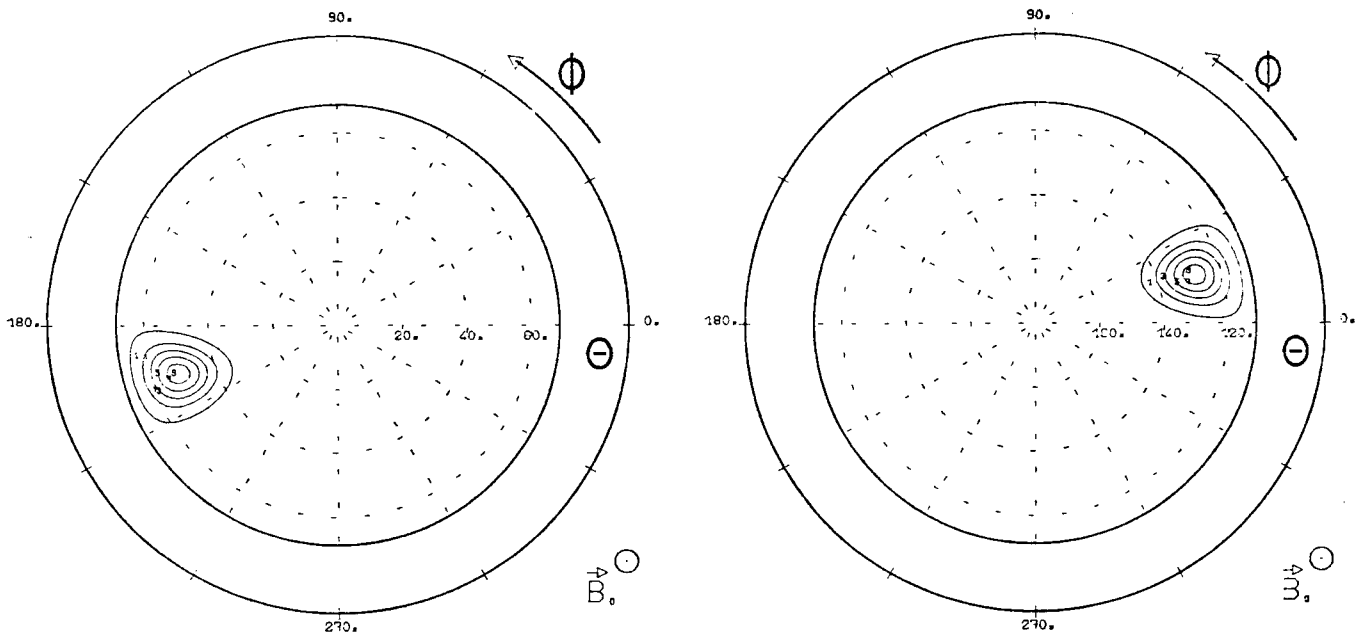

FIG.10

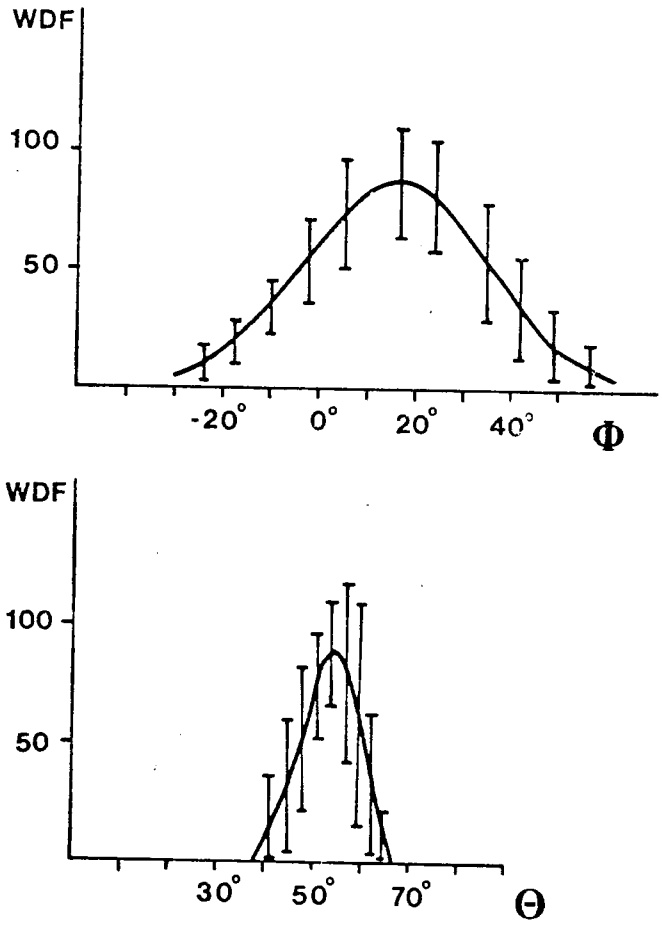

FIG.11

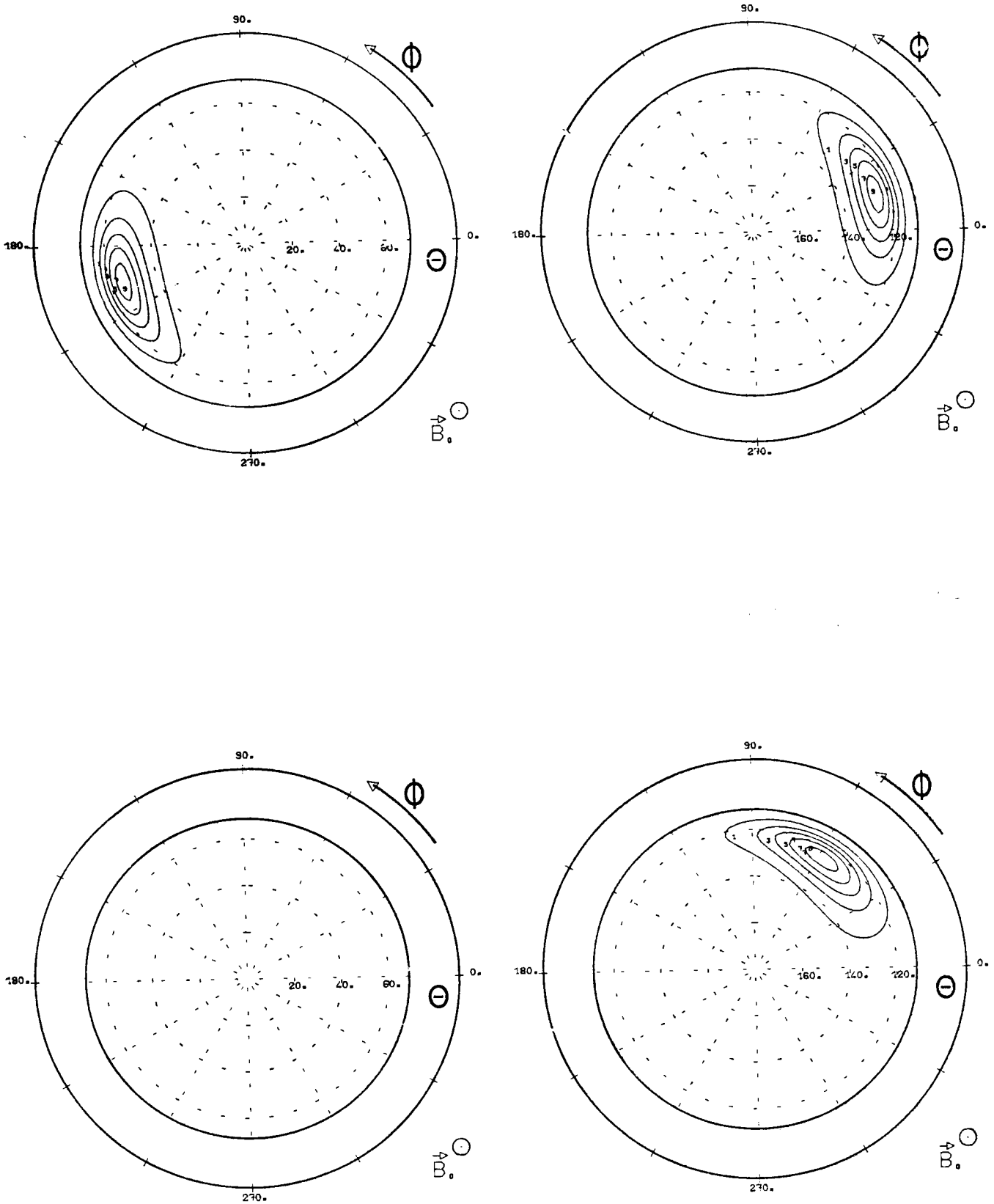

FIG.12

NOTES CRPE - DIFFUSION

- C.N.E.T., 38-40 Rue du Général Leclerc - 92131 ISSY LES MOULINEAUX
  - . M. Maurice BERNARD, (Direction) 1 ex.
  - . M. LE MEZEC (DICET) 1 ex.
  - . M. PROFIT (Direction) 1 ex.
  - . M. DUBOS (PARIS B) 1 ex.
  - . S.D.I./DIP Bibliothèque 1 ex.
- R.P.E. -
  - . I. REVAH 1 ex.
  - . P. BAUER 1 ex.
  - . Bibliothèque 2 ex.
  - (Circulation Chefs de Groupe) + 1 ex.
- C.N.E.T. Lannion - Bibliothèque - Route de Trégastel 22300 LANNION 1 ex.
- C.R.P.E. - - C.N.R.S. 45045 ORLEANS CEDEX
  - . J. HIEBLOT 1 ex.
  - . Bibliothèque 2 ex.
  - (Circulation Chefs de Groupe) + 1 ex.
- L.G.E. - 4 Avenue de Neptune - 94100 ST MAUR DES FOSSES
  - . Bibliothèque 1 ex.
- C.N.R.S. Bibliothèque Service "Rapports" à l'Attention de Mme CARROLL - 26, rue Boyer - 75791 PARIS Cédex 20 1 ex.
- C.N.E.S. - 129 rue de l'Université - 75007 PARIS 1 ex.
- I.N.A.G. - 17 Avenue Denfert Rochereau - 75014 PARIS 1 ex.
- I.U.T. BOURGES - 18 Avenue de Lattre de Tassigny - 18000 BOURGES
  - . MM. RENARD Claude, GIRARDEAU MONTAUT J.P. 2 ex.
- DR. C.A. REDDY, Head of Space Physics Division - Vikram Sarabhai Space Centre, Trivandrum 695022 - India 1 ex.
- Pr. Satya PRAKASH - Physical Research Laboratory Navrangura Ahmedabad 380009 - India 1 ex.
- Pr. A.K. GHATAK - Department of Physics - Indian Institute of Technology - New Delhi 110029 - India 1 ex.
- Directeur C.E.S.R. - B.P. 4057 - 31029 TOULOUSE 1 ex.
- E.S.A. - Melle G. SPATZ - Service Documentation Spatiale 8-10 rue Mario Nikis - 75738 PARIS Cédex 15 1 ex.
- Directeur C.E.P.H.A.G. - B.P. 15 - 38040 GRENOBLE Cédex 1 ex.
- François LEFEUVRE CRPE/CNET/CNRS ORLEANS 30 ex.
- Michel PARROT " 13 ex.
- T. NEUBERT Danish Space Research Institute LYNGBY Denmark 30 ex.

CRPE
Centre de Recherches
en Physique de l'Environnement
terrestre et planétaire

Avenue de la Recherche scientifique
45045 ORLEANS CEDEX

Département PCE
Physique et Chimie
de l'Environnement

Avenue de la Recherche scientifique
45045 ORLEANS CEDEX

Département ETE
Etudes par Télédétection
de l'Environnement

CNET - 38-40 rue du général Leclerc
92131 ISSY-LES-MOULINEAUX

CNET imp 75/1163